Scale-Dependent Evaluation of Seamless Short-Term Forecasts of Convective Precipitation

Martin Rempel Markus Schultze [1] Ulrich Blahak [1]

[1]Deutscher Wetterdienst, Offenbach, Germany

Within the DWD project SINFONY (Seamless INtegrated FOrecastiNg sYstem), the combined forecasting system INTENSE (INTegration of NWP Ensembles and Extrapolations) was developed, which provides seamless precipitation forecasts up to 12 h ahead. In terms of domain-wide and time-averaged verification metrics, the forecasts generated by INTENSE ideally combine precipitation nowcasting and NWP. However, the accurate and consistent forecasting of small-scale structures like convective cells is important in meteorological and hydrological warning management. With objects defined as contiguous precipitation structures and identified by the object analysis tool tobac (Heikenfeld et al., 2019) we have assessed size-dependent systematic errors of ICON-D2-RUC forecasts and quantified geometric object properties statistically to identify inconsistencies within the transition period of INTENSE.

Introducing INTENSE

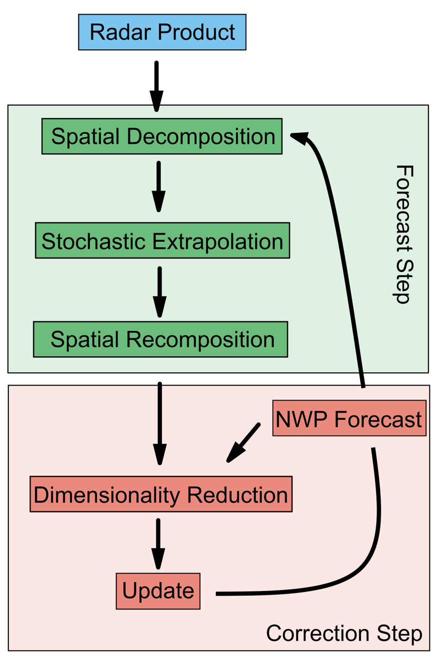

Figure 1. Scheme of the INTENSE approach. The latest available radar products (blue) provide the basis for the STEPS-DWD algorithm (green). Forecasts are iteratively corrected by use of NWP data (red).

Algorithm

INTENSE represents an adapted and enhanced version of a combination method published by Nerini et al., 2019. Here, various radar products (reflectivity, QPE) can be used as input (Fig. 1; blue). These observational products are extrapolated by the scheme of STEPS-DWD (Rondinel et al., 2022; green) that is used as a forward model in the sense of data assimilation. The correction step is carried out in the dimensionality-reduced PCA space (red). Thus, in each 5 min forecast step the extrapolation is corrected by ICON-D2-RUC data iteratively. To reduce non-gaussianity, areas without precipitation are replaced and transformed, which further reduces the need for a probability matching as a post-processing step.

Objectives

- What determines the time it takes for INTENSE forecasts to converge towards the NWP forecast?
- Do objects identified in INTENSE forecast exhibit inconsistencies in their properties compared to those identified in radar observations and NWP-based simulated reflectivities?

Dataset & Verification Results Based on FSS

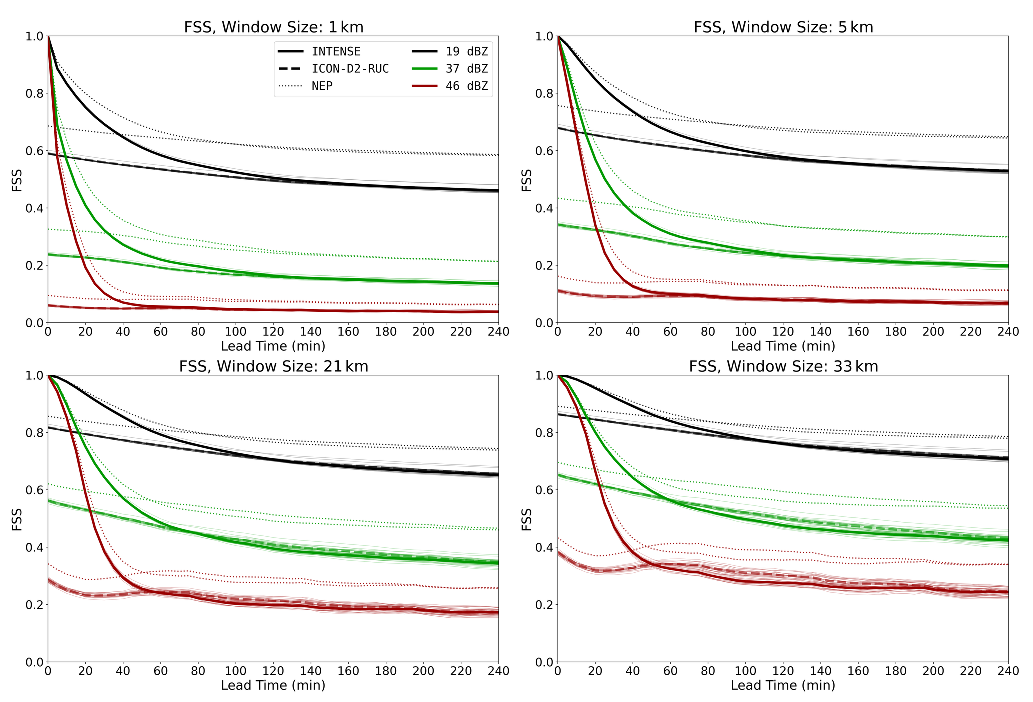

Figure 2. Average FSS scores for INTENSE (solid lines) and ICON-D2-RUC (dashed lines). Thin solid lines represent FSS curves of each ensemble member. The curve of neighborhood ensemble probability (NEP) is shown as bold dashed line

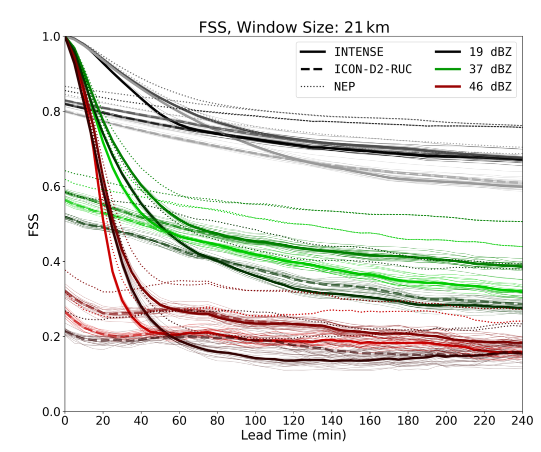

Figure 3. Same as Fig. 2, but divided in categories of different convergence times.

Dataset

35 casedays of 2023 for which hourly INTENSE forecasts up to 4 h are used. Pure STEPS-DWD extrapolations are not considered.

FSS

The average FSS reveals a smooth transition towards the forecast quality of ICON-D2-RUC for small window sizes (Fig. 2). For larger window sizes and reflecitivities >37 dBZ, an underestimation is visible that is mainly caused by forecast with a convergence time around 180 min (Fig. 3).

Ensemble Spread for Different Convergence Times

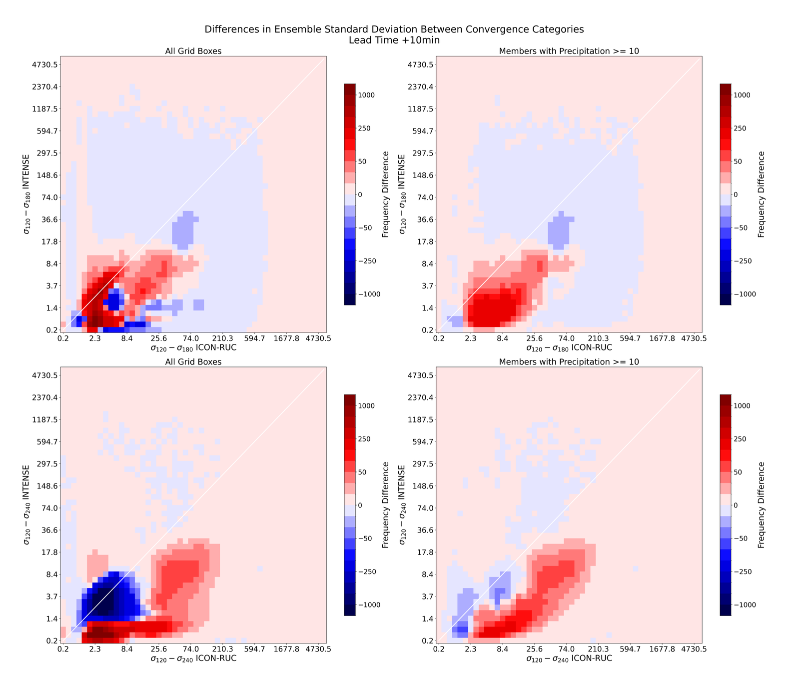

Figure 4. Differences in ensemble variance structures between forecasts with a convergence time of 120 min and those with a time of 180 min (upper row) and 240 min (bottom row), respectively, for all grid boxes (left) and grid boxes at which at least ten ensemble member have precipitation (right).

Ensemble Variance Structure

Two cases are compared for the ensemble variance structure to highlight the effects of rainless area replacement. First, the ensemble variance at all grid boxes is computed. Second, only grid boxes are included in the computation at which both ensembles forecast rainfall in at least ten members. Here, positive values indicate variances that are dominant in cases with a convergence time of around 120 min. Therefore, INTENSE has a shorter convergence time when a large spread occurs in the NWP ensemble in areas where also INTENSE predicts precipitation. If there is a large spatial error between INTENSE and ICON-D2-RUC, rainless area replacement lead to an increase in convergence times (s. blue regions in Fig. 4).

Object-Based Evaluation of INTENSE

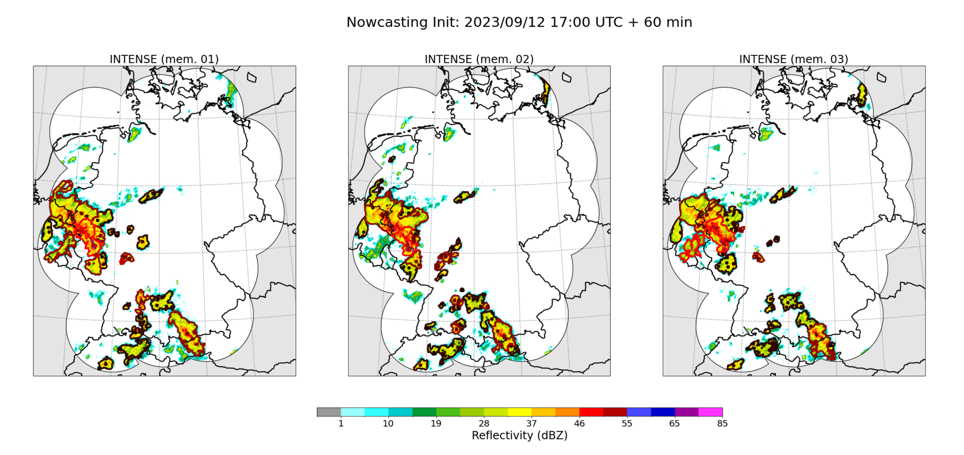

Figure 5. The first three members of an exemplary 60 min INTENSE forecast valid for 12th September 2023 18 UTC. Reddish contours depict the identified objects in different threshold categories.

Approach

tobac (Heikenfeld et al., 2019) was utilized for object identification & tracking. Objects werde identified on different threshold levels (37, 46, 55 dBZ) and a weighted distance from threshold was used to locate object centers. Investigated were distributions of the size-resolved number of objects and area covered by precipitation for different lead times.

Further investigated are size-resolved rank histograms for geometric properties of objects between observation and INTENSE for the first forecast hour as well as the lifetime of objects existing at forecast start.

Number Size Distributions and Geometric Properties

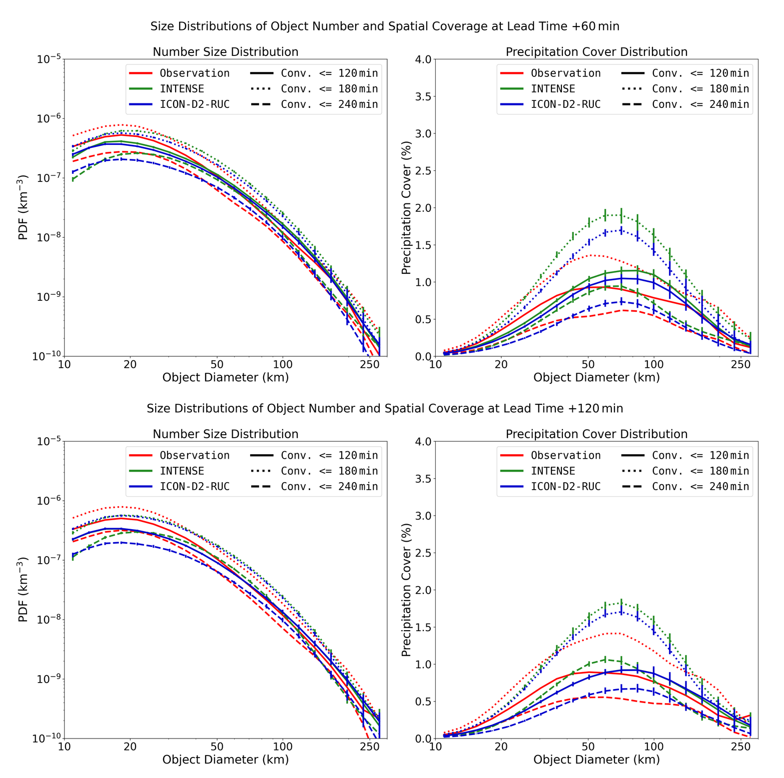

Figure 6. Object number size distribution (left) and precipitation cover distribution (right) for +60 min (top) and +120 min (bottom) divided in different convergence categories.

Number Size Distribution

Number size distributions of ICON-D2-RUC and INTENSE forecasts reveal an overestimation of very small and large objects in all three considered convergence categories. Further, this underestimations increases with lead time. However, medium cells with a diameter between 50 and 100 km are overestimated.

Precipitation Cover Distribution

This positive bias can also be seen in precipitation cover distribution. Here, medium-sized objects lead to most of the precipitation coverage in the investigated period. For individual convergence time categories, the expected value for short convergence times is slightly shifted towards larger objects backing the assumption that a larger union of areas with precipitation leads to a shorter convergence time.

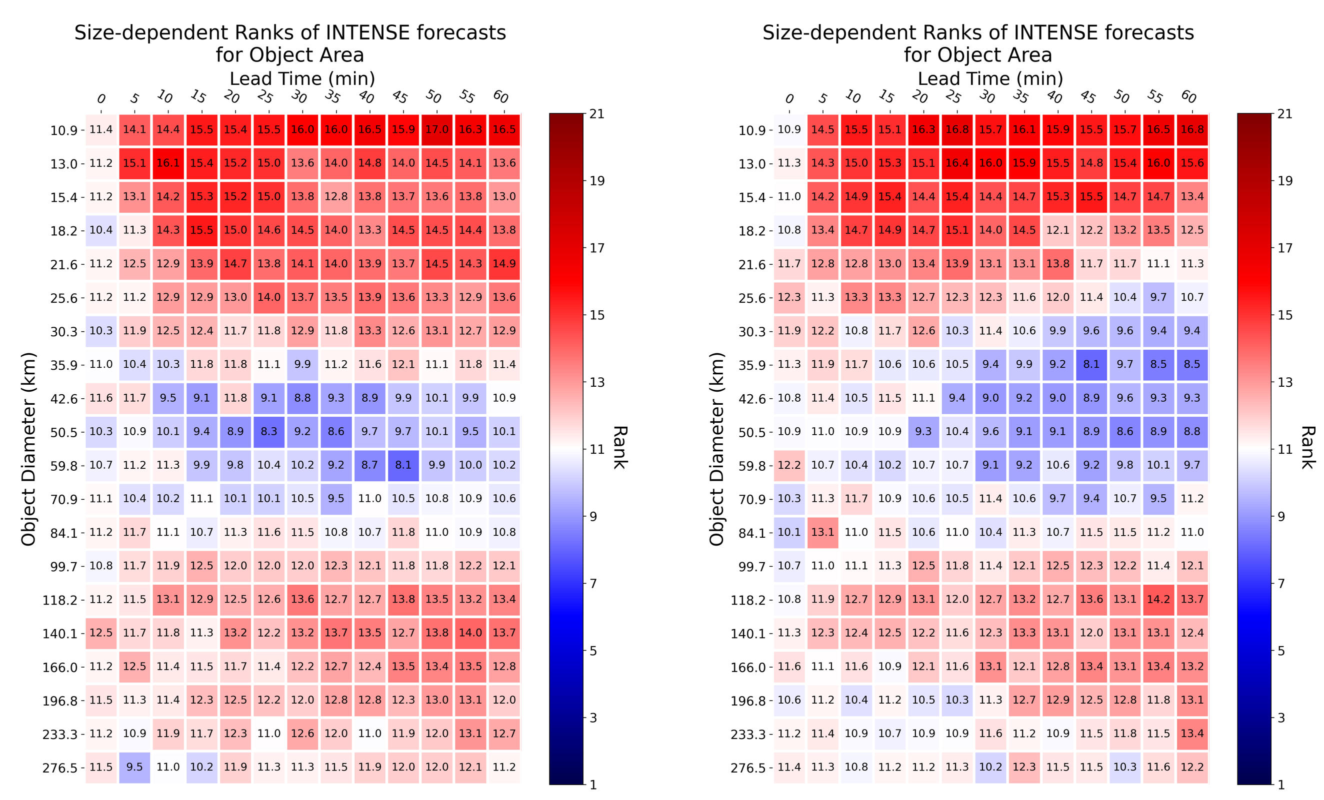

Figure 7. Averaged rank histograms for object areas in the first hour of INTENSE forecasts are shown for forecast with a convergence time of around 120 min (left) and with a convergence time of 240 min (right).

Size-Resolved Rank Histograms

To further investigate the deviations in precipitation cover of INTENSE forecasts shown above, size-resolved rank histograms are used showing the first hour of an INTENSE forecast. Blueish colors reveal an overestimation of the ensemble, since the observation meets lower values of the sorted ensemble, while reddish colors reveal an underestimation. Both categories show the development of the overestimation for medium cells. However, it is more distinct for a convergence time of 240 min (cf. Fig. 6).

Object Lifetimes

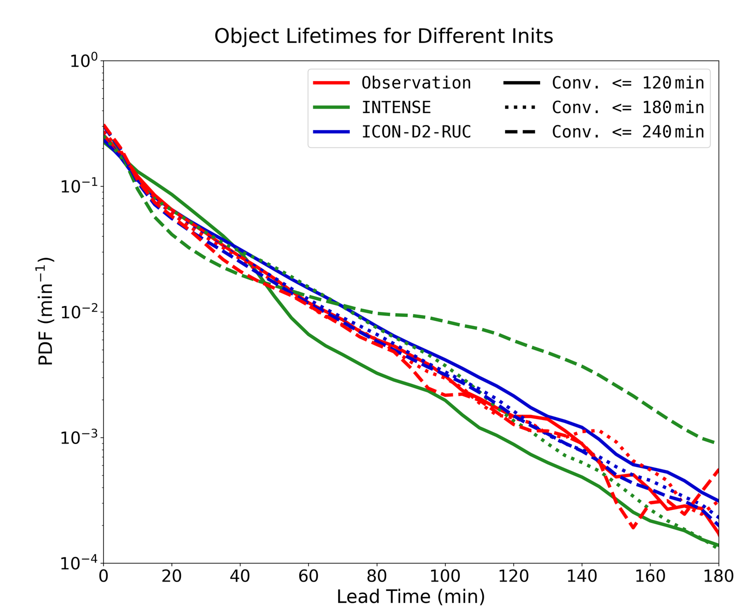

Figure 8. Lifetime distribution of objects that are existing at the beginning of an INTENSE forecast for the observation (red), ICON-D2-RUC (blue), and INTENSE (green) as well as for different convergence times.

Object Lifetimes

Fig. 8 shows object lifetimes for the observation as well as for forecasts of INTENSE and ICON-D2-RUC. While lifetimes of NWP-based objects are comparable with obserevd ones, INTENSE reveal differences for short and long convergence times. For former objects with a lifetime between 20-40 min are more frequent, while more persistent cells are underestimated. This may an indicator for inconsistencies in the transition region from observation towards the NWP. On the other hand, for longer convergence times, INTENSE reveal a strong overestimation of long-living cells while objects with a short lifetime are underrepresent. This may attributable to smoothing effects leaving only a few dominant long-living precipitation structures.